Title

ortho-Aromatic polyamides by ring-opening polymerization of N-carboxyanhydrides

Journal

Chem, 11(5)

ISSN

1925-6981

Authors

Deng, Shijie
Jung, Hyuk-Joon
Shen, Yi
et al.

Publication Date

2025-05-01

DOI

10.1016/j.chempr.2024.12.004

Chem

CellPress

Article

ortho-Aromatic polyamides by ring-opening polymerization of *N*-carboxyanhydrides

Shijie Deng,[1,5] Hyuk-Joon Jung,[1,5] Yi Shen,[1] Hootan Roshandel,[1] Varit Chantranuwathana,[1] Hieu D. Nguyen,[2] Thi V. Tran,[2] Kimberly Vasquez,[1] Joseph Chang,[3] Takeo Iwase,[3] Parisa Mehrkhodavandi,[3] Jeffery A. Byers,[4] Loi H. Do,[2] and Paula L. Diaconescu[1,6,*]

[1]Department of Chemistry and Biochemistry, University of California, Los Angeles, Los Angeles, CA 90095, USA

[2]Department of Chemistry, University of Houston, Houston, TX 77004, USA

[3]Department of Chemistry, University of British Columbia, Vancouver, BC V6T 1Z1, Canada

[4]Department of Chemistry, Boston College, Chestnut Hill, MA 02467, USA

[5]These authors contributed equally.

[6]Lead contact

*Correspondence: pld@chem.ucla.edu

SUMMARY

Among major engineering plastics, aromatic polyamides are high-performance materials with high mechanical strength and heat resistance. However, the production of these materials is limited to para- and meta-aromatic polyamides via polycondensation leading to polymers with low molecular weight and high dispersity. Here, we report the ring-opening polymerization of *N*-alkylated aromatic six-membered ring *N*-carboxyanhydrides (6-NCA-R) catalyzed by transition metal Schiff base complexes in the presence of a base. This system allows the facile synthesis of ortho-aromatic polyamides with high molecular weights via chain-growth polymerization. A mechanism is proposed based on the results of polymerizations performed under various reaction conditions. In addition, the tunability of polymer solubility and thermal properties are shown by varying the length of *N*-alkyl side chains, and copolymerization of 6-NCA-R with heterocyclic monomers is performed to prepare heteroatom (N, O, and S) containing copolymers. These findings provide a synthetic pathway for functional polyamide materials with tailored properties for various applications.

Aromatic polyamide, *N*-carboxyanhydride, isatoic anhydride, ring-opening polymerization, Schiff base metal complex.

INTRODUCTION

Aromatic polyamides are extra tough and flame-resistant materials with a wide range of applications owing to the rigid nature of the backbone and strong intermolecular attractions.[1-3] Despite these eminent properties, their high melting temperature and poor solubility lead to difficulties in processing.[4] Consequently, flexible pendant groups are employed to modify the properties of aromatic polyamide by reducing their rigidity and chain interaction.[5] In addition, the introduction of alkyl groups to the nitrogen atoms in the backbone significantly expands the range of chemical variations that can be achieved in aromatic poly- and oligoamides, making them an important group of abiotic foldamers.[6-8] While para and meta substrates have been investigated, examples of ortho-aromatic polyamides remain rare. Hamilton and coworkers reported that the presence of intramolecular hydrogen bonds in ortho-benzamide oligomers leads to a planar arrangement of substituents and promotes the formation of linear strand structures.[9] Alkylation of the nitrogen atom would disrupt these hydrogen bonds, allowing an increased

THE BIGGER PICTURE

The world is almost unimaginable without plastics given their wide range of applications. Despite the rising environmental concerns, they still have massive potentials as materials. Thus, various polymers that are functional as well as degradable have been developed for advanced applications. Accordingly, the development of new catalytic systems that can polymerize various monomers selectively is important and necessary. Aromatic polyamides are high-performance materials due to their excellent mechanical properties, however, ortho-aromatic polyamides were inaccessible to date because suitable catalytic systems have not been developed. Herein, we report a metal-catalyzed ring-opening polymerization of *N*-carboxyanhydrides as a new synthetic pathway to ortho-aromatic polyamides with high molecular weights, and their copolymers. These findings offer a new strategy to develop advanced polyamide materials with tailored properties.

chemical diversity and the possibility of tuning cis/trans isomerization based on steric and electronic interactions.

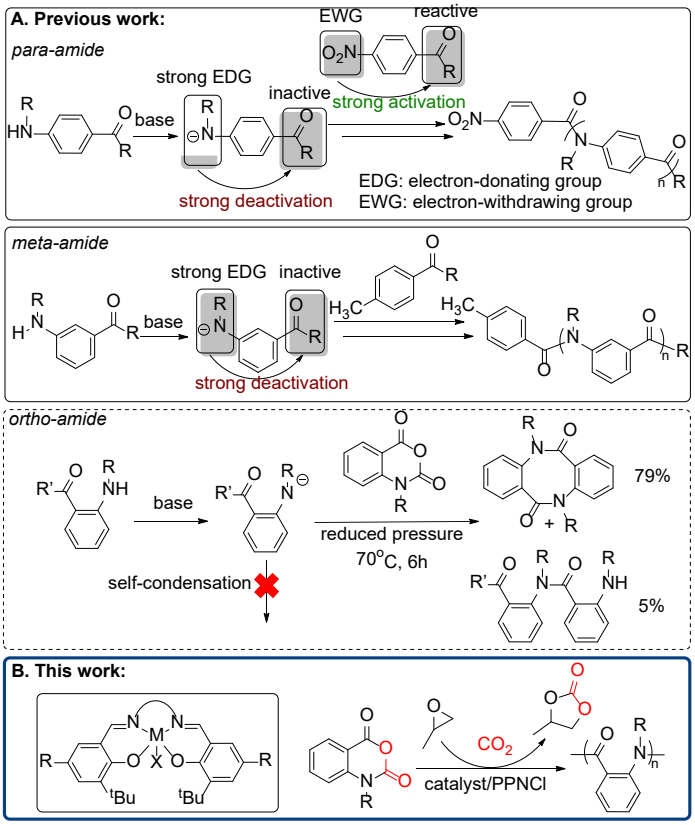

Scheme 1. Synthesis of aromatic polyamides

(A) Chain-growth polymerization for the synthesis of para[10] and meta[11] aromatic polyamides was reported by Yokozawa and coworkers, but the same strategy does not apply to ortho-aromatic polyamides.[12]

(B) Ring-opening polymerization for the synthesis of ortho-aromatic polyamides is reported in this work.

The synthesis of aromatic polyamides (Scheme 1), however, is generally limited to polycondensation reactions that lead to polymers with low molecular weight and broad dispersity.[13,14] In 2000, Yokozawa and coworkers reported a strategy that used a base to deactivate monomers and a reactive initiator to optimize the condensation reaction.[10,11,15,16] Similarly, in 2021, Kiblinger and coworkers reported another activation strategy that showed good control over the polycondensation reaction.[17] However, these methods were only effective for para and meta-aromatic polyamides. Furthermore, while Yokozawa and coworkers showed the formation of ortho-amides from the reaction of deprotonated *N*-alkylanthranilic acid ester and *N*-alkylisatoic anhydride in the presence of a base, the polymerization reaction to form polyamides did not occur,[12] and the synthesis of ortho-aromatic polyamides remains challenging.

Although the ring-opening polymerization of *N*-carboxyanhydrides (NCAs) has been investigated in polyamide synthesis as an alternative route to polycondensation reactions,[18-23] aromatic β-NCAs, such as isatoic anhydride and its derivatives, have not been employed before. Thus, the synthesis of polyamides via the ring-opening polymerization of aromatic β-NCAs is an unexplored synthetic route due to the absence of a suitable catalytic system.

Given our previous success with using metal complexes for the ring-opening polymerization of cyclic esters and ethers,[24-39] we decided to apply a similar system to NCA polymerization. Herein, we report the first example of successful ring-opening polymerization of aromatic β-NCAs to prepare ortho-aromatic polyamides using Schiff base metal complexes, [PPN]Cl

([PPN]$^+$ = bis(triphenylphosphoranylidene)iminium), and propylene oxide. High molecular weight ortho-aromatic polyamides were obtained from β-NCA monomers with different *N*-alkyl side chains, allowing the further characterization of a new class of polyamides. We also propose a mechanism for the ring-opening polymerization of aromatic β-NCAs. Similar systems were previously exploited in the ring-opening copolymerization of epoxides and anhydrides,[40,41] ring-opening copolymerization of epoxides and dihydrocoumarin,[42] coupling reactions between CO_2 and epoxides,[43,44] as well as the ring-opening polymerization of *S*-carboxyanhydrides.[45] The homopolymerization of α-NCAs by Schiff base metal complexes for polypeptide synthesis was also reported.[46]

RESULTS

Metal-catalyzed ring-opening polymerization of aromatic β-NCAs for the synthesis of ortho-aromatic polyamides

The polymerization of 5-membered-ring NCAs can be initiated by primary amines, whereas the aromatic 6-membered-ring NCAs exhibit significantly lower reactivity. Our attempts to use an aromatic primary amine, *p*-phenylenediamine,[47,48] as an initiator for 6-NCA-R polymerization led to no reaction (Table S4, entry 1). Consequently, the polymerization of aromatic 6-membered-ring NCAs necessitates the development of a suitable catalytic system.

We started by adapting reaction conditions from reported five-membered-ring NCA polymerizations[46] using a ferrocene-based aluminum complex.[36] An equivalent of (salfen)AlO^{i}Pr (**Al-1,** salfen = *N,N′*-bis(2,4-di-*tert*-butylphenoxy)-1,1′-ferrocenediimine), 2 equivalents of [PPN]Cl, 50 equivalents of 6-NCA-Bn (Bn = benzyl), and propylene oxide (PO) as the solvent were used (Table 1, entry 1). The reaction mixture was heated at 80 °C for 2 hours, resulting in the formation of an off-white precipitate. Notably, the resulting solid was only slightly soluble in trifluoroacetic acid (TFA), while being insoluble in solvents such as tetrahydrofuran (THF), methylene chloride, dimethylformamide, or dimethyl sulfoxide. We speculated that the product obtained was a polymer, but our characterization was limited due to its low solubility. To address this issue, we attempted to increase the polymer solubility by using monomers with longer *N*-alkyl side chains. Therefore, we synthesized 6-NCA-C_8H_{17} (NCA-8), an analogue with an *N*-octyl group, and used it as a monomer (Table 1, entry 2). Using the same reaction conditions as described above, we obtained poly(NCA-8) with a significantly improved solubility, allowing us to acquire its ^{1}H and ^{13}C NMR spectra in $CDCl_3$ (Figure 1A). The integration of peaks in the ^{1}H NMR spectrum is consistent with the structure of poly(NCA-8).

The polymer peaks in the ^{1}H NMR spectrum appeared broader compared to those of the corresponding NCA monomer (Figure 1A). Particularly, the broad and multiple -NCH_2- peaks of the polymer, which are labeled "e" in Figure 1A, were observed in the range of 3.15 to 5.10 ppm due to the presence of both *cis* and *trans* conformations of the amide bond in the polymer backbone.[49,50] A variable temperature ^{1}H NMR study of the polymer showed the peak interchange within that range as the temperature increased from 30 to 110 °C (Figure S23). The polymer displayed a *cis* conformational preference at 30 °C, however, an increase in the *trans* conformation was observed at higher temperatures due to the rotation around the amide bonds. When the ^{1}H NMR spectrum of the polymer was obtained in a mixture of CF_3COOD and $CDCl_3$, the peaks of the *trans* conformation were significantly enhanced (Figure S24), likely because the protonated carbonyl group of the amide bond could form a C=N bond, thus inhibiting the rotation around the amide bonds, and leading to a *trans* conformational preference.

Additionally, during the course of the NCA-8 polymerization, the formation of propylene carbonate was observed by ^{1}H NMR spectroscopy (Figure S26). As the conversion of monomer increased over time, the yield of propylene carbonate increased accordingly, and eventually an almost quantitative yield (94.2%) for propylene carbonate was observed in 2 hours. This suggests that as soon as CO_2 is generated from the NCA polymerization process, the transformation of released CO_2 into propylene carbonate takes place simultaneously. A mechanism is proposed below (Scheme 2). The formation of cyclic carbonate was also observed when Schiff base metal compounds together with [PPN]Cl and PO were employed in the 5-membered ring NCA polymerization.[46]

Table 1. Ring-opening polymerization of 6-NCA-R[a]

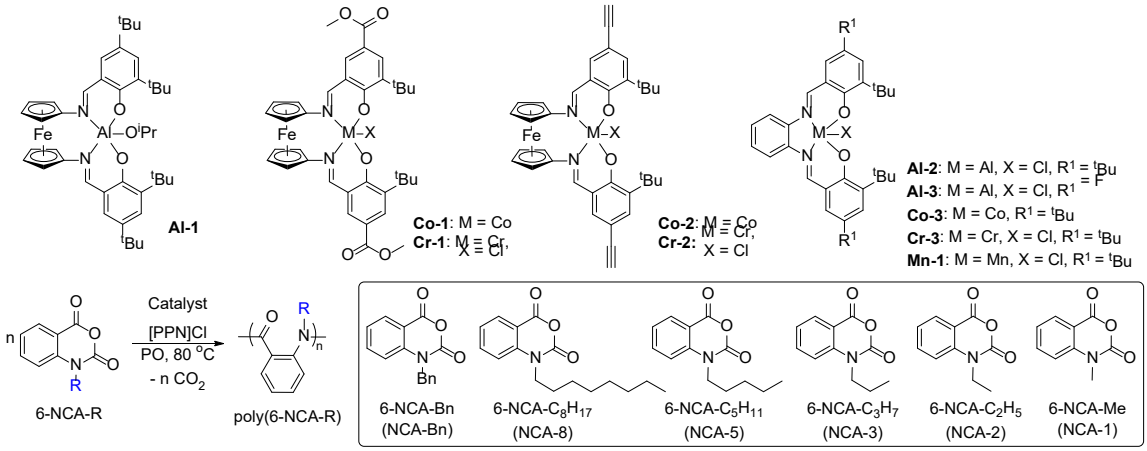

	Cat.	6-NCA-R	[cat]:[cocat]:[M]	Solv.	Temp. (°C)	Time (h)	Yield (%)[b]	$M_{n,theo}$ (kDa)[c]	$M_{n,SEC}$ (kDa)[d]	$Đ^d$	I (%)[e]
1	**Al-1**	NCA-Bn	1:2:50	PO	80	2	86	-	-[j]	-[j]	-
2	**Al-1**	NCA-8	1:2:50	PO	80	2	74	8.7	38.1	1.33	22.8
3	**Co-1**	NCA-8	1:2:50	PO	80	2	92	10.7	16.8	1.33	63.7
4	**Cr-1**	NCA-8	1:2:50	PO	80	2	85	9.9	29.2	1.45	33.9
5	**Co-2**	NCA-8	1:2:50	PO	80	2	99	11.5	24.4	1.48	47.1
6	**Cr-2**	NCA-8	1:2:50	PO	80	2	96	11.2	24.7	1.56	45.3
7	**Al-2**	NCA-8	1:2:50	PO	80	2	83	9.7	25.3	1.33	38.3
8	**Co-3**	NCA-8	1:2:50	PO	80	2	60	7.0	22.4	1.29	31.3
9	**Cr-3**	NCA-8	1:2:50	PO	80	2	30	3.6	8.4	1.26	42.9
10	**Mn-1**	NCA-8	1:2:50	PO	80	2	60	7.0	17.6	1.22	39.8
11	**Al-2**	NCA-8	1:0:50	PO	80	24	0	-	-	-	-
12	**Al-2**	NCA-8	0:2:50	PO	80	2	49	5.7	38.6	1.65	14.8
13	**Al-2**	NCA-8	1:1:50	PO	80	2	70	8.2	25.9	1.38	31.7
14	**Al-2**	NCA-8	1:5:50	PO	80	2	74	8.7	18.5	1.23	47.0
15[f]	**Al-2**	NCA-8	1:2:50	PO	80	2	48	5.6	23.0	1.18	24.3
16[g]	**Al-2**	NCA-8	1:2:50	THF	80	2	89	10.4	105	1.57	9.9
17[h]	**Al-2**	NCA-8	1:2:50	THF	80	2	18	2.2	31.2	1.47	7.1
18[i]	**Al-2**	NCA-8	1:2:50	THF	80	43	0	-	-	-	-
19[g]	**Al-2**	NCA-8	1:2:100	THF	80	4	64	14.9	125	1.61	11.9
20[g]	**Al-2**	NCA-8	1:2:200	THF	80	7	29	13.5	206	1.64	6.6
21	**Al-2**	NCA-8	1:2:50	CHO	80	2	0	-	-	-	-
22	**Al-2**	NCA-8	1:2:50	CHO	80	24	90	10.5	34.6	1.40	30.3
23	**Al-2**	NCA-8	1:2:50	PO	50	4	65	7.6	22.0	1.25	34.5
24	**Al-2**	NCA-8	1:2:50	PO	25	24	11	1.4	12.7	1.16	11.0
25	**Al-3**	NCA-8	1:1:50	PO	80	22	79	9.2	28.0	1.33	32.9
26	**Al-2**	NCA-8	1:2:25	PO	80	1	65	3.9	20.8	1.21	18.8
27	**Al-2**	NCA-8	1:2:100	PO	80	4	90	20.9	32.2	1.35	64.9
28	**Al-2**	NCA-8	1:2:200	PO	80	7	86	40.0	44.5	1.41	89.9
29	**Al-2**	NCA-8	1:2:400	PO	80	20	79	73.2	77.3	1.64	94.7
30	**Al-2**	NCA-5	1:2:50	PO	80	2	90	8.6	19.3	1.21	44.6
31	**Al-2**	NCA-3	1:2:50	PO	80	2	94	7.7	25.6	1.12	30.1
32	**Al-2**	NCA-2	1:2:50	PO	80	2	90	6.7	22.6	1.12	29.6
33	**Al-2**	NCA-1	1:2:50	PO	80	2	89	-	-[j]	-[j]	-

[a]All polymerizations were carried out using 4 μmol precatalyst and 0.6 mL solvent.
[b]Polymer yields were determined gravimetrically.
[c]$M_{n,\,theo}$ =([6-NCA-R]$_0$/[Cat]) × (MW of 6-NCA-R - MW of CO_2) × polymer yield + MW of epoxide + Cl + H.
[d]M_n and Đ were determined by SEC-MALS measurements in THF.

[e]Initiation efficiency = ($M_{n,theo}/M_{n,SEC}$)×100
[f]Polymerization was carried out with [PPN]OBz.
[g]Polymerization was carried out in THF with 100 equiv of PO.
[h]Polymerization was carried out in THF with 10 equiv of PO.
[i]Polymerization was carried out in THF with 0 equiv of PO.
[j]Insoluble polymer products were obtained.

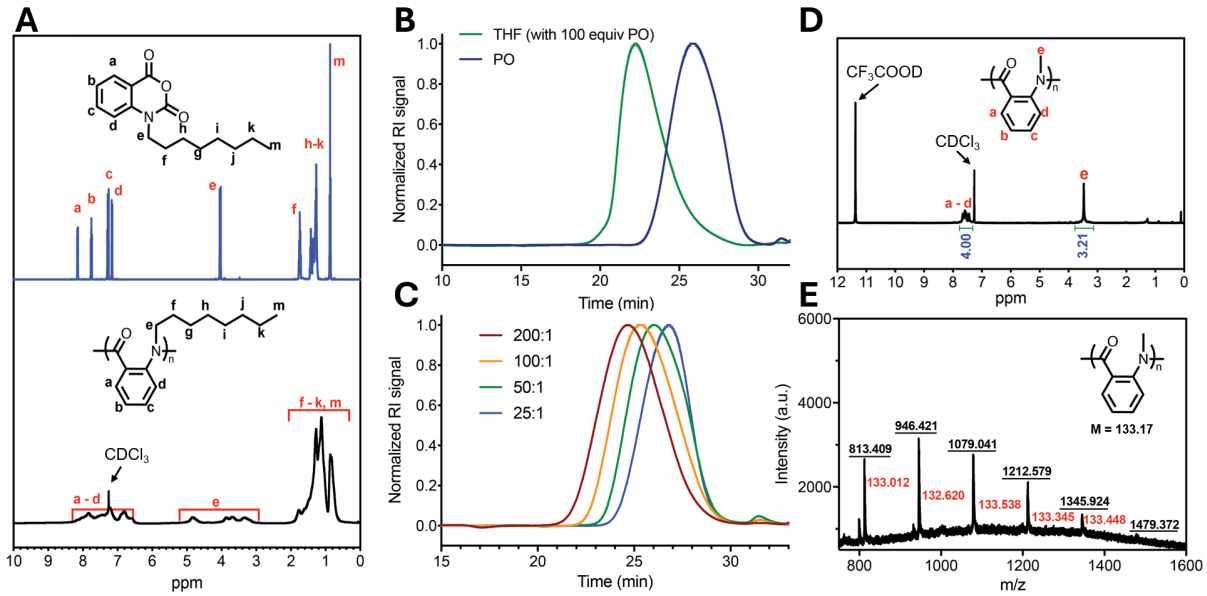

Figure 1. ortho-Aromatic polyamides from ring-opening polymerization of 6-NCA-R

(A) ^{1}H NMR (500 MHz, 25 °C) spectra of NCA-8 (top) and poly(NCA-8) (bottom) in $CDCl_3$.
(B) SEC traces of polymer obtained from using THF as the solvent with 100 equiv of PO added (green; Table 1, entry 16) and using neat PO (blue; Table 1, entry 7).
(C) SEC traces of the polymers obtained with varying the [NCA-8]:[cat] feed ratio (Table 1, entries 7, 26-28).
(D) ^{1}H NMR (500 MHz, 25 °C) spectrum of poly(NCA-1) (Table 1, entry 33) in $CDCl_3$:CF_3COOD = 5:1.
(E) MALDI-TOF-MS of poly(NCA-1) (Table 1, entry 33).

Catalyst screening for ring-opening polymerization of 6-NCA-R

To investigate the effect of ligand design and metal center on the polymerization rate and the properties of the resulting polymers, we tested several other ferrocene-based metal compounds for NCA-8 polymerization. The structures were chosen based on our previous studies of other reactions[51] and known cobalt and chromium systems that displayed high activity in conjunction with [PPN]Cl in ring-opening polymerization/copolymerization,[52-54] and other reports on the coupling of CO_2 and epoxides.[44,55-57]

Two cobalt complexes, **Co-1** ((salfen^{COOMe})Co, salfen^{COOMe} = dimethyl 5,5'-((1*E*,1'*E*)-(ferrocene-1,2-diylbis(azaneylylidene))bis(methaneylylidene))bis(3-(*tert*-butyl)-4-hydroxybenzoate)) and **Co-2** ((salfen^{CCH})Co, salfen^{CCH} = 6,6'-((1*E*,1'*E*)-(ferrocene-1,2-diylbis(azaneylylidene))bis(methaneylylidene))bis(2-(*tert*-butyl)-4-ethynylphenol)), demonstrated high activity. The polymer obtained using **Co-1**, with an ester group at the para position of the aryloxide ring, displayed a molecular weight closer to the expected value and narrower molecular weight distribution than **Co-2**, with alkyne groups in the same position (Table 1, entry 3 vs. 5). In the case of chromium compounds, **Cr-1**, an analogue of **Co-1**, polymers with a higher molecular weight and narrower molecular weight distribution were obtained compared to **Cr-2**, an analogue of **Co-2** (Table 1, entry 4 vs. 6).

Our major goal with the metal compounds bearing a ferrocene backbone was to achieve the redox switchable copolymerization[24-39] of NCA-8 and PO. Therefore, we started with an equivalent of (salfen)AlO^iPr (**Al-1**), 2 equivalents of [PPN]Cl, 50 equivalents of NCA-8, and PO as a solvent. After heating at 80 °C for 0.5 hours to allow partial conversion (the reduced

Al-1 does not polymerize epoxides), ^{Ac}FcBAr^{F} (^{Ac}Fc = acetylferrocene, BAr^{F} = tetrakis(3,5-bis(trifluoromethyl)phenyl) borate) was added to oxidize **Al-1** and initiate the polymerization of PO (Figure S27). Unfortunately, only the poly(NCA-8) homopolymer was isolated at the end. We also attempted to initiate the polymerization with the oxidized form of **Al-1**. However, upon the addition of the [PPN]Cl cocatalyst, the decomposition of the oxidized aluminum compound was observed, as evidenced by the color change from dark red to orange, and the formation of a black precipitate. The decomposition was attributed to the incompatibility between the ferrocenium backbone and the chloride anion.[58]

Given the lack of redox switchable copolymerization, we then turned to metal compounds supported by a simple salph ligand (salph = *N,N'*-bis(3,5-di-*tert*-butylsalicylidene)-1,2-diaminobenzene) to study the role of the metal compound, [PPN]Cl, and PO in NCA-8 polymerization. The aluminum compound (salph)AlCl (**Al-2**) demonstrated comparable activity to **Al-1**, and showed a higher yield of polymer and improved control of molecular weight compared to **Al-1** (Table 1, entry 7). We also prepared a series of analogous transition metal compounds, (salph)Co (**Co-3**),[59] (salph)CrCl (**Cr-3**),[59] and (salph)MnCl (**Mn-1**),[60] for comparison. Although these metal compounds exhibited a similar control of polymer molecular weight under the same reaction conditions, the polymer yields were significantly curtailed in comparison with **Al-2** (Table 1, entries 8-10). Therefore, we chose to carry out further reactions with **Al-2**.

Role of each component in the catalytic system

We first investigated the role of the [PPN]Cl cocatalyst. Generally, bis(triphenylphosphine)iminium salts ([PPN]X) are widely used as versatile cocatalysts to form active catalysts and achieve high activity in various polymerizations. The ratio of cocatalyst to metal catalyst varies for optimal polymerization conditions, and the [cocatalyst]/[metal catalyst] ratio can be higher than 1.[61,62] In a control experiment using only **Al-2** without [PPN]Cl, no polymerization was observed (Table 1, entry 11). However, when [PPN]Cl was used alone without the aluminum compound, the polymerization still occurred at a slower rate with a lower initiation efficiency, resulting in a higher polymer molecular weight and dispersity compared to when the aluminum compound was present (Table 1, entry 12). These findings suggest the importance of both the aluminum compound and the [PPN]Cl cocatalyst for the formation of the active species and controlling the polymerization. Then, we changed the amount of [PPN]Cl from 2 to 1 to 5 equivalents (Table 1, entries 13-14). The reduced amount of cocatalyst led to a lower yield of polymer and initiation efficiency, while at higher cocatalyst loadings, a better control of polymer molecular weight but lower yield of polymer were observed. When another cocatalyst, [PPN]OBz (OBz^{-} = benzoate), was employed instead of [PPN]Cl, a lower polymer yield and initiation efficiency were observed (Table 1, entry 15). Therefore, 2 equivalents of [PPN]Cl was used for further polymerization of different NCA monomers, in agreement with other reports.[44,45]

To investigate the effect of the PO amount on initiation efficiency, we proceeded to conduct the polymerization using THF as a solvent and used PO as an additive to the reaction mixture to initiate the polymerization and trap the CO_2 released. Interestingly, when the polymerization was performed in THF with 100 equivalents of PO, the polymerization rate remained relatively unchanged, with a polymer yield of 89% after 2 hours (Table 1, entry 16). However, a significantly increased molecular weight of the resulting polymer was observed (105 kDa), while the polymer yield was similar to that obtained in neat PO (Table 1, entry 7), indicating a much lower initiation efficiency (9.9%). The polymerization in THF with 10 equivalents of PO exhibited a very low yield of polymer (18%) and initiation efficiency (7.1%, Table 1, entry 17). Eventually, no polymerization occurred at all in THF without PO, suggesting PO is essential to initiate the polymerization (Table 1, entry 18). All polymers, obtained from the polymerizations with 50 equivalents of monomer either using THF with PO or using neat PO, exhibited monomodal size exclusion chromatography (SEC) traces (Figure S53, S61-62). Specifically, the trace from the polymerization in neat PO displayed a shift toward a lower molecular weight as a result of high initiation efficiency (Figure 1B). Further investigation into the use of THF as a solvent revealed that the polymerizations with higher monomer feed ratios produced high molecular weight polymers (Table 1, entries 19-20). However, the yield of polymer decreased significantly as the monomer feed ratio increased, and the corresponding SEC traces displayed bimodal molecular weight

distributions (Figure S63-64). These results suggest that the polymerization needs to be performed in neat PO for optimal results.

We also attempted the polymerization in neat cyclohexene oxide (CHO) to investigate whether PO may be replaced with another epoxide (Table 1, entries 21-22). Eventually, the polymerization in neat CHO with an extended reaction time demonstrated a comparable molecular weight and dispersity of resulting polymer, and initiation efficiency to that in neat PO (Table 1, entry 7). However, no polymer was obtained from the polymerization in neat CHO in 2 hours, indicating a slower polymerization rate.

Control experiments were performed to verify that this system is inert toward PO, cyclohexene oxide (CHO), and propylene carbonate (PC, Table S3, entries 1-3). Importantly, none of these substrates was polymerized under the same reaction conditions employed for the NCA polymerization. In addition, the formation of polycarbonate by copolymerization of in situ generated CO_2 and epoxide was not observed over the NCA polymerization. The selective formation of polyamide is attributed to a low CO_2 pressure and high reaction temperature, suppressing the formation of polycarbonate, which is in agreement with other similar catalyst systems.[44,63-66]

All polymerizations were conducted in a sealed Schlenk tube at 80 °C. Since the reaction temperature is higher than the boiling point of PO, as commonly adopted for other polymerizations in neat PO,[42,67,68] the effect of reaction temperature on the NCA polymerization was evaluated. In comparison with the polymerization at 80 °C (Table 1, entry 7), the polymerization at 50 °C (Table 1, entry 23) showed a similar initiation efficiency while the yield of polymer decreased even with a prolonged reaction time. However, the polymerization at room temperature (Table 1, entry 24) exhibited a significantly reduced yield of polymer (11%) and initiation efficiency (11.0%) after 24 hours, suggesting that a reaction temperature higher than 50 °C is necessary for efficient polymerizations.

Instead of carrying out the polymerization in a sealed system, with a reaction under bubbling argon gas was performed to evaluate the activity in an open system. The reaction conditions of Table 1, entry 17 were adopted to minimize the use of PO and investigate whether the removal of CO_2 by argon gas enhances the polymerization. However, no polymer was obtained from the open system, indicating that the polymerization in a sealed system with neat PO is an effective way of polymerization (Table S5).

To further optimize the catalytic system and achieve better control over the polymerization process, we employed a fluorinated salph aluminum compound, (salph-F)AlCl (**Al-3**). Coates and coworkers previously reported that **Al-3** can effectively suppress side reactions such as transesterification and epimerization in the copolymerization of propylene oxide and different cyclic anhydrides.[68] However, in our case, the NCA-8 polymerization with **Al-3** was significantly slower than that with **Al-2**, and no major differences were observed in the polymer molecular weight and dispersity (Table 1, entry 13 vs. 25).

We also varied the monomer feed ratio to investigate the effect of monomer concentration on initiation efficiency (Table 1, entries 26-29). As the monomer feed ratio increased, the determined molecular weight of resulting polymers increased accordingly (Figure 1C). Importantly, the trend in the determined molecular weights showed that the polymer molecular weight became closer to the theoretical value at a higher monomer concentration. The good match between experimental and theoretical molecular weights suggests a greater initiation efficiency at higher monomer loadings, resulting in a well-controlled polymerization behavior. Monitoring the molecular weight and dispersity of polymers from the polymerization of 100 equivalents of NCA-8 with 2 μmol **Al-2**, 4 μmol [PPN]Cl, and 0.6 mL PO at 80 °C further confirmed the controlled characteristics of this system. The molecular weight of polymers increased linearly over time, while the dispersity of polymers remained relatively constant throughout the reaction (Figure S76).
In addition to the polymerization of NCA-8, we also achieved the polymerization of different 6-NCA-R monomers in 2 hours regardless of the identity *N*-alkyl side chain length (Table 1, entries 30-33). These results show the versatility of the system used.

Proposed mechanism for the ring-opening polymerization of 6-NCA-R

Based on the results of our studies, we propose a mechanism for the ring-opening polymerization of 6-NCA-R (Scheme 2). Considering that **Al-2** is inactive toward NCAs in the absence of the cocatalyst [PPN]Cl and PO, two routes for the formation of the active species may be envisioned. A neutral aluminum alkoxide, (salph)Al(OR), generated by the insertion of PO into an Al–Cl bond reacts further with the iminium salt to form a monoalkoxide species, (salph)Al(OR)(Cl)$^-$. Alternatively, (salph)AlCl$_2^-$ is generated first from the reaction of **Al-2** and iminium salt, followed by a ring opening of PO by a chloride to form the same monoalkoxide species. Since all SEC traces of obtained polymers are monomodal, and the NCA polymerization cannot be initiated without [PPN]Cl and PO, the active species initiating NCA polymerization is likely the monoalkoxide species; the bisalkoxide species, (salph)Al(OR)$_2^-$, may be produced in low quantities under similar conditions.[41,69,70] End group analysis by matrix-assisted laser desorption/ionization time-of-flight mass spectrometry (MALDI-TOF-MS) confirmed the presence of an alkoxy end group generated from a ring opening of PO by a chloride (Figure S82). In addition, the alkoxy end group from [PPN]OBz was also observed by MALDI-TOF-MS analysis when [PPN]OBz was used as a cocatalyst (Figure S83). Therefore, the initiation step involves a ring opening of NCA by the alkoxide bound to Al in the active species. After the initiation, the subsequent decarboxylation process releases CO_2 to form an Al–N bond that could attack another NCA. Then, the propagation step proceeds by repeating the ring opening of NCA and decarboxylation process until terminated by methanol.

CO_2 released in situ during propagation can be inserted into an Al–O bond of the monoalkoxide species. Then, the intramolecular backbiting of metal-bound carbonate occurs to produce cyclic carbonates and regenerate the monoalkoxide species for further CO_2 trapping.[71] The relatively low molecular weight distributions of the obtained polymers and initiation efficiencies of the polymerizations at a low monomer concentration ($Đ$ = 1.12–1.33; 29.6–44.6%; Table 1, entries 7, 30-32) suggest that CO_2 insertion into free Al monoalkoxide species is faster than an additional initiation of NCA polymerization by the free Al monoalkoxide species once CO_2 is generated. Importantly, the formation of cyclic diamide that Yokozawa and coworkers previously reported was not observed in our system (Scheme 1),[12] likely because the Al–N bond is not nucleophilic enough to attack the non-activated carbonyl carbon between the benzene ring and the oxygen atom in free NCA to form an amide linkage.

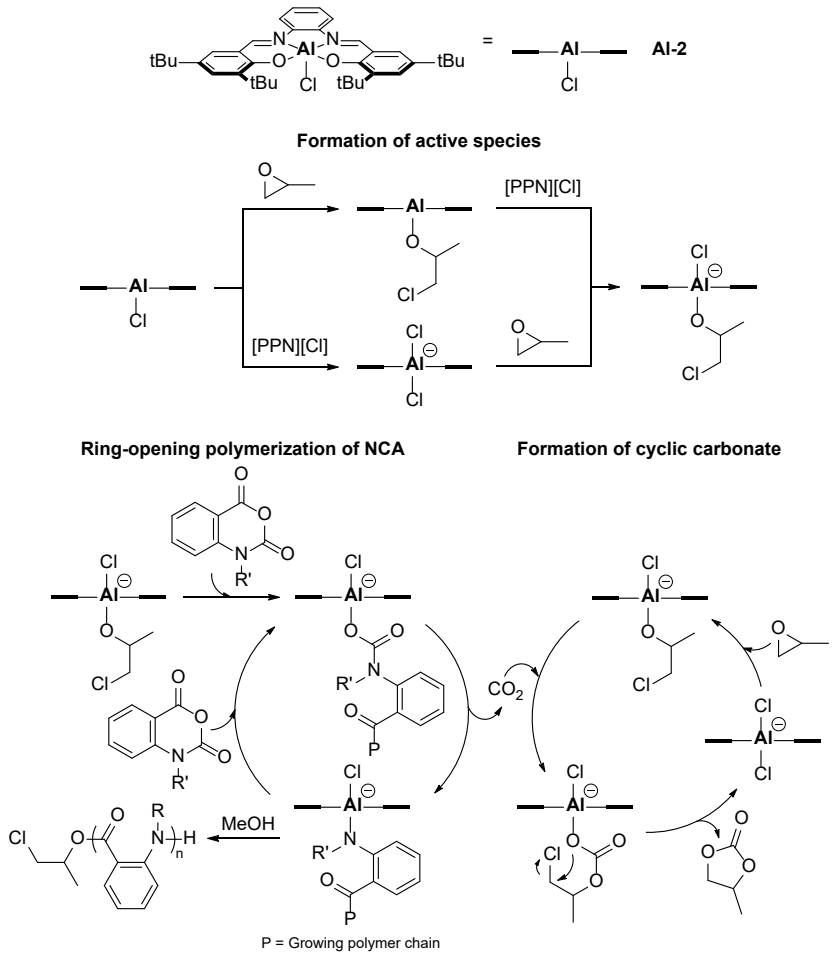

Scheme 2. Proposed mechanism for the formation of ortho-aromatic polyamides and cyclic carbonate

The proposed mechanism shows the initiating species forms polyamide and cyclic carbonate ([PPN]$^+$ moiety in the aluminate species is omitted for clarity).

Copolymerization of 6-NCA-R with heterocyclic monomers

In addition to homopolymerizations, the block copolymerization of two different NCA monomers by sequential addition was attempted to confirm the presence of an active chain end (Table 2, entries 1-2). As the first monomer, NCA-8, was polymerized at 80 °C for the first 2 hours, the reaction mixture was cooled down to room temperature to add a second NCA monomer (NCA-5 or NCA-2), followed by heating again at 80 °C for another 2 hours. In both cases, the resulting polymers had molecular weights close to the corresponding theoretical molecular weights, and their SEC traces were monomodal (Figure S77-78). The ^{1}H NMR spectra of the block copolymers indicated that the ratio of the two NCA units in their structure is almost 1:1 (Figure S28 and 30).

Table 2. Copolymerization of 6-NCA-R with various heterocyclic monomers

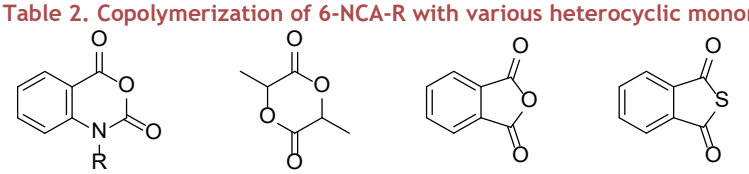

NCA-8 (R = C_8H_{17})
NCA-5 (R = C_5H_{11})
NCA-2 (R = C_2H_5)
NCA-1 (R = C_1H_3)

rac-LA

PA

PTA

	M1	M2	Yield (%)[c]	$M_{n,theo}$ (kDa)[d]	$M_{n,SEC}$ (kDa)[e]	$Đ$[e]	M1:M2[f]
1[a]	NCA-8	NCA-5	48	10.2	9.3	1.31	1:1.02
2[a]	NCA-8	NCA-2	54	10.3	12.0	1.34	1:0.97
3[a]	NCA-8	*rac*-LA[g]	34	17.1	10.7	1.10	1:0.08
4[b, h]	NCA-8	PA	80	35.1	26.0	1.37	1:1.08
5[b]	NCA-1	PA	82	-	-[i]	-[i]	1:1.59
6[b, h]	NCA-1	PTA	45	16.1	7.5	1.14	1:1.77

[a]Sequential block copolymerizations were carried out at 80 °C using 4 μmol **Al-2**, 0.6 mL PO. [**Al-2**]$_0$:[PPNCl]$_0$:[M1]$_0$:[M2]$_0$ = 1:2:50:50. Reaction times: NCA (2 h) and lactide (3 h).

[b]One-pot copolymerizations were carried out at 80 °C using 4 μmol **Al-2**, 1.2 mL PO. [**Al-2**]$_0$:[PPNCl]$_0$:[M1]$_0$:[M2]$_0$ = 1:2:100:100. Reaction times: NCA and PA (2 h), NCA and PTA (6 h).

[c]Polymer yields were determined gravimetrically.

[d]$M_{n,\,theo}$ = ((MW of 1st NCA - MW of CO_2) × [1st NCA]$_0$/[Cat] + (MW of 2nd NCA - MW of CO_2) × [2nd NCA]$_0$/[Cat]) × polymer yield + MW of epoxide + Cl + H. For lactide copolymerization, $M_{n,\,theo}$ = (MW of NCA - MW of CO_2) × [NCA]$_0$/[Cat] + (MW of lactide) × [lactide]$_0$/[Cat] × conversion of lactide + MW of epoxide + Cl + H. For cyclic anhydride copolymerization, $M_{n,\,theo}$ = ((MW of NCA - MW of CO_2) × [NCA]$_0$/[Cat] + (MW of cyclic anhydride + MW of PO) × [cyclic anhydride]$_0$/[Cat]) × polymer yield + MW of epoxide + Cl + H.

[e]M_n and $Đ$ were determined by SEC-MALS measurements in THF.

[f]Ratio of each monomer unit in the resulting copolymer.

[g]Conversion of lactide was determined by ^{1}H NMR spectroscopy.

[h]SEC trace showed a multimodal molecular weight distribution.

[i]Insoluble polymer products were obtained.

In addition, diffusion ordered NMR spectroscopy (DOSY) experiments showed that all components of the obtained polymers diffused at the same rate, suggesting the formation of block copolymers (Figure S40-41). For example, the DOSY of the NCA-8 and NCA-2 block copolymer displayed clearly distinguishable resonance peaks corresponding to the side chains of NCA-8 and NCA-2 at 4.82 and 3.82 ppm, respectively, and these peaks diffused together with other resonance peaks.

Similarly, the sequential block copolymerization of NCA-8 and *rac*-lactide (*rac*-LA) was attempted (Table 2, entry 3). The conversion of lactide after 3 hours was 75%, however, the ^{1}H NMR spectrum of the purified block copolymer showed that the degree of lactide incorporation was only 7.5% (Figure S32), likely due to the competing homopolymerization of *rac*-lactide initiated by residual aluminum alkoxide species. The resulting polymer had a monomodal molecular weight distribution (Figure S79), and its DOSY plot displayed a single peak on the y axis with resonances assigned to poly(NCA-8) and polylactide at 5.19 ppm, indicating the formation of a block copolymer (Figure S42).

Furthermore, a one-pot copolymerization of NCA and a cyclic anhydride requiring a similar initiating system was performed. The heterocyclic monomer mixture was heated at 80 °C in the presence of **Al-2**, [PPN]Cl, and PO. The resulting polymer from the copolymerization of NCA-8 and phthalic anhydride (PA) exhibited a molecular weight similar to that expected, but with a multimodal molecular weight distribution, likely due to the different reactivity of these monomers (Table 2, entry 4, Figure S80). The ^{1}H NMR spectrum of the polymer indicated a 1:1 composition ratio between NCA and PA units (Figure S34), and DOSY confirmed the formation of a copolymer consisting of amide and ester units (Figure S43).

As the homopolymer of NCA-1 was readily soluble only in TFA, the substrate scope was expanded to NCA-1 with PA and phthalic thioanhydride (PTA) to evaluate the capability of this system to prepare a copolymer of polyamide and polyester/polythioester that would improve the solubility of poly(NCA-1) in common organic solvents (Table 2, entries 5-6). While the polymers obtained from the copolymerization of NCA-1 and PA were still insoluble in $CHCl_3$ and THF, changing the comonomer from PA to PTA led to the resulting polymers being soluble in $CHCl_3$, CH_2Cl_2, and THF, allowing further characterization. Unlike the copolymerization of NCA-8 and PA, the polymers from both copolymerizations exhibited more cyclic anhydride units in their structure rather than maintaining the initial monomer ratio, likely due to the poor solubility of NCA-1 (Figure S36 and 38). The formation of the desired copolymers was confirmed by DOSY (Figure S44-45). Despite the low-molecular-

weight copolymer of NCA-1 and PTA owing to the residual phthalic acid that was generated during the synthesis of PTA and acted as a chain transfer reagent,[72] these results suggest that this system can provide synthetic pathways to heteroatom (N, O, and S) containing polymers.

Tunable physical and thermal properties of polyamide homo- and copolymers

Returning to polyamide homopolymers, we varied the chain length to investigate the influence of the *N*-alkyl side chain length on solubility and thermal properties (Table 1, entries 30-33). Previous studies have shown that *N*-alkylated poly(*p*-benzamide)s are only soluble in THF when the alkyl chain length is no shorter than heptyl.[73] On the other hand, *N*-alkylated poly(*m*-benzamides) generally exhibit better solubility, with even the *N*-methyl polymer being soluble in THF.[74] In our current study, we focused on poly(6-NCA-R), which is *de facto* poly(*o*-benzamide). Interestingly, the solubility of poly(6-NCA-R) falls between its para and meta counterparts. We found that poly(6-NCA-R) with alkyl chains as short as an ethyl group was soluble in THF (Table S1). Poly(NCA-1) is soluble in TFA and only slightly soluble in methylene chloride and chloroform. Therefore, the ^{1}H NMR spectrum of poly(NCA-1) was obtained in a $CF_3COOD/CDCl_3$ mixture, which showed peak integrations matching the structure of an *N*-methyl aromatic polyamide (Figure 1D). The polymer structure was further confirmed by MALDI-TOF-MS, in which the spacing between adjacent peaks was consistent with the molar mass of the *N*-methyl aromatic amide repeating unit (Figure 1E).

The thermal properties of the poly(6-NCA-R) polymers were characterized by thermal gravimetric analysis (TGA) and differential scanning calorimetry (DSC) (Table S2). The polymers all demonstrated high thermal stability. For example, poly(NCA-8) showed a $T_{d,5\%}$ (temperature at 5% weight loss) as high as 395 °C when heated at a scan rate of 5 °C/min under a nitrogen atmosphere (Figure 2A). This thermal stability is comparable to its para counterpart, which has a $T_{d,5\%}$ at 417 °C.[73] Given that the poly(6-NCA-R) polymers have similar $T_{d,5\%}$ values (Figure S84-87), the thermal stability seems to be determined by the nature of the backbone instead of the length of the side chain. The second heating DSC curve of poly(NCA-8) revealed a melting temperature T_m of 213 °C (Figure 2B). For previously reported *N*-alkylated poly(*p*-benzamides), the decrease in *N*-alkyl chain length caused an increase in the melting temperature of the polymer; however, poly(NCA-5), poly(NCA-3), poly(NCA-2), and poly(NCA-1) showed no melting transitions within the temperature window of -50 to 300 °C (Figure S95-98).[73] Although the *N*-alkylated poly(*p*-benzamide)s did not show every thermal transition from DSC analysis either, the 3rd heating DSC curves in the range of 30 to 400 °C were further collected for poly(NCA-5), poly(NCA-3), poly(NCA-2), and poly(NCA-1) in case additional thermal transitions can be observed in the high-temperature range. While a T_g of poly(NCA-1) was newly observed at 106 °C (Figure S99), we were not able to determine T_g values for the rest of the polymers due to weak thermal transitions, as also reported for *N*-alkylated poly(*p*-benzamide).[73] In addition, no T_m was observed in the high-temperature range, suggesting that the T_m of poly(6-NCA-R) with short side chains is close to its T_d or that thermal decomposition occurs before melting.

In comparison with homopolymers, the TGA and DTG curves of block copolymers consisting of two different NCA monomer units showed a slightly lowered $T_{d,5\%}$ at 337 °C, and almost the same T_{max} (temperature of maximum peak) at 444 °C, respectively (Figure S88-89). This suggests that the polyamide block copolymers have similar thermal stability regardless of the identity of NCA comonomers due to the same backbone structure. However, copolymers of NCA and cyclic anhydrides displayed two-step degradations on TGA curves, which were reflected in two T_{max} values on the DTG curves, implying that the copolymers have a gradient structure rather than a random distribution of each monomer unit (Figure S91-93). The thermal transition of the NCA-8 homopolymer was clearly observed from the DSC analysis, however, the DSC curves of block copolymers with NCA-8 units exhibited weak T_m and T_c signals, owing to the formation of block copolymers (Figure S100-102). The copolymers of NCA with PA and PTA had T_g at 46 and 63 °C, respectively (Figure S103-105). These values are attributable to segments of PA and PTA units given that the reported T_g values of poly(PA-*alt*-PO) and poly(PTA-*alt*-PO) are 46 and 63 °C, respectively.[72]

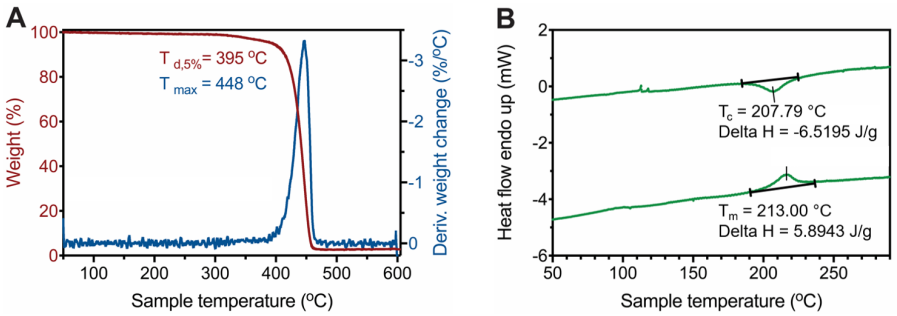

Figure 2. Thermal characterization of poly(NCA-8)

(A) Thermogravimetric analysis (TGA) and derivative thermogravimetry (DTG) curves of poly(NCA-8).

(B) The second heating (bottom) and cooling (top) curves of differential scanning calorimetry (DSC) thermograms for poly(NCA-8) (Table 1, entry 7).

The powder X-ray diffraction (PXRD) patterns were further collected to verify the crystallinity of the polymers (Figure S106-110). All poly(6-NCA-R), except poly(NCA-8), showed minor diffraction peaks at 26, 37, and 40 ° in 2θ, however, there were not many other peaks and the intensity of peaks was low, indicating the polymers are amorphous materials with some loosely packed crystalline domains. This is generally attributed to the rigid backbone of aromatic polyamides makes crystallization difficult. Considering the PXRD pattern of poly(NCA-8) with unclear broad peaks, the rest of the polymers with shorter side chains likely form minor lattices without disturbance of the steric hindrance from side chains. In addition, this observation suggests the octyl substituents in poly(NCA-8) are not long enough to crystalize by themselves.

Conclusions

In conclusion, we successfully developed a catalytic system consisting of a Schiff base metal compound, [PPN]Cl, and propylene oxide for the polymerization of 6-NCA-R to *N*-alkylated ortho-aromatic polyamides. This is the first example of high molecular weight ortho-aromatic polyamide synthesis via ring-opening polymerization of β-NCA. Through the investigation of each component's role in the catalytic system, we were able to propose a mechanism for the polymerization of 6-NCA-R and achieve improved control over the polymerization process. Additionally, we were able to tune the polymer solubility and thermal properties by varying the length of the *N*-alkyl chain as well as prepare heteroatom (N, O, and S) containing polymers by copolymerization of NCA and heterocyclic monomers. Overall, this study provides insight into the synthesis and characterization of *N*-alkylated ortho-aromatic polyamides, offering control over their solubility and thermal properties through rational design and optimization of the catalytic system and monomer structure. These findings open up new possibilities for the development of advanced polyamide materials with tailored properties for various applications.

EXPERIMENTAL PROCEDURES

Resource availability

Lead contact

Further information and requests for resources should be directed to and will be fulfilled by the lead contact, Paula L. Diaconescu (pld@chem.ucla.edu).

Materials availability

All materials used in this study and full experimental details can be found in the supplemental information.

Data and code availability

All data needed to evaluate the conclusions in the paper are present in the paper and/or the supplemental information.

SUPPLEMENTAL INFORMATION

Supplemental information includes experimental details, NMR spectra, UV-Vis spectra, SEC traces, MALDI-TOF spectra, TGA traces, DSC traces, and PXRD patterns.

ACKNOWLEDGMENTS

We thank the National Science Foundation as part of the Center for Integrated Catalysis (CHE-2023955) for supporting this work. S. Deng and Y. Shen are grateful for INFEWS fellowships (NSF Grant DGE-1735325). We acknowledge Dr. Matthew Thompson from Boston College for insightful discussions.

AUTHOR CONTRIBUTIONS

S.D. and H.-J.J. contributed equally by designing and performing the experiments. P.L.D. supervised the project. S.D., H.-J.J., and P.L.D. co-wrote the manuscript. All authors participated in synthesis and characterization of metal compounds and polymers.

DECLARATION OF INTERESTS

The authors declare no competing interests.

REFERENCES

1. Yang, B., Wang, L., Zhang, M., Luo, J., Lu, Z., and Ding, X. (2020). Fabrication, Applications, and Prospects of Aramid Nanofiber. Adv. Funct. Mater. *30*, 2000186. 10.1002/adfm.202000186.
2. Coste, M., Suárez-Picado, E., and Ulrich, S. (2022). Hierarchical Self-assembly of Aromatic Peptide Conjugates into Supramolecular Polymers: It Takes Two to Tango. Chem. Sci. *13*, 909-933. 10.1039/D1SC05589E.
3. Sobiech, T.A., Zhong, Y., and Gong, B. (2022). Cavity-containing Aromatic Oligoamide Foldamers and Macrocycles: Progress and Future Perspectives. Org. Biomol. Chem. *20*, 6962-6978. 10.1039/D2OB01467J.
4. García, J.M., García, F.C., Serna, F., de la Peña, J.L. (2010). High-performance aromatic polyamides. Prog. Polym. Sci. *35*, 623-686. 10.1016/j.progpolymsci.2009.09.002.
5. Ruiz, J.A.R., Trigo-Lopez, M., García, F.C., García, J.M. (2017). Functional Aromatic Polyamides. Polymers *9*, 44. 10.3390/polym9090414.
6. Zhang, D.-W., Zhao, X., Hou, J.-L., and Li, Z.-T. (2012). Aromatic Amide Foldamers: Structures, Properties, and Functions. Chem. Rev. *112*, 5271-5316. 10.1021/cr300116k.
7. Akhdar, A., Gautier, A., Hjelmgaard, T., and Faure, S. (2021). N-Alkylated Aromatic Poly- and Oligoamides. ChemPlusChem *86*, 298-312. 10.1002/cplu.202000825.
8. Li, Z., Cai, B., Yang, W., and Chen, C.-L. (2021). Hierarchical Nanomaterials Assembled from Peptoids and Other Sequence-Defined Synthetic Polymers. Chem. Rev. *121*, 14031-14087. 10.1021/acs.chemrev.1c00024.
9. Hamuro, Y., Geib, S.J., and Hamilton, A.D. (1996). Oligoanthranilamides. Non-Peptide Subunits That Show Formation of Specific Secondary Structure. J. Am. Chem. Soc. *118*, 7529-7541. 10.1021/ja9539857.
10. Yokozawa, T., Ogawa, M., Sekino, A., Sugi, R., and Yokoyama, A. (2002). Chain-Growth Polycondensation for Well-Defined Aramide. Synthesis of Unprecedented Block Copolymer Containing Aramide with Low Polydispersity. J. Am. Chem. Soc. *124*, 15158-15159. 10.1021/ja021188k.
11. Sugi, R., Yokoyama, A., Furuyama, T., Uchiyama, M., and Yokozawa, T. (2005). Inductive Effect-Assisted Chain-Growth Polycondensation. Synthetic Development from para- to meta-Substituted Aromatic Polyamides with Low Polydispersities. J. Am. Chem. Soc. *127*, 10172-10173. 10.1021/ja052566z.
12. Yokoyama, A., Karasawa, M., Taniguchi, M., and Yokozawa, T. (2013). Successive Formation of Two Amide Linkages between Two Benzene Rings. Chem. Lett. *42*, 641-642. 10.1246/cl.130143.
13. Alizadeh, M., and Kilbinger, A.F.M. (2018). Synthesis of Telechelic Poly(p-benzamide)s. Macromolecules *51*, 4363-4369. 10.1021/acs.macromol.8b00587.
14. Reese, C.J., Qi, Y., Abele, D.T., Shlafstein, M.D., Dickhudt, R.J., Guan, X., Wagner, M.J., Liu, X., and Boyes, S.G. (2022). Aromatic Polyamide Brushes for High Young's Modulus Surfaces by Surface-Initiated Chain-Growth Condensation Polymerization. Macromolecules *55*, 2051-2066. 10.1021/acs.macromol.1c02088.
15. Yokozawa, T., Asai, T., Sugi, R., Ishigooka, S., and Hiraoka, S. (2000). Chain-Growth Polycondensation for Nonbiological Polyamides of Defined Architecture. J. Am. Chem. Soc. *122*, 8313-8314. 10.1021/ja001871b.
16. Yokozawa, T., and Ohta, Y. (2016). Transformation of Step-Growth Polymerization into Living Chain-Growth Polymerization. Chem. Rev. *116*, 1950-1968. 10.1021/acs.chemrev.5b00393.
17. Pal, S., Nguyen, D.P.T., Molliet, A., Alizadeh, M., Crochet, A., Ortuso, R.D., Petri-Fink, A., and Kilbinger, A.F.M. (2021). A Versatile Living Polymerization Method for Aromatic Amides. Nat. Chem. *13*, 705-713. 10.1038/s41557-021-00712-3.
18. Deming, T.J. (1997). Facile Synthesis of Block Copolypeptides

of Defined Architecture. Nature *390*, 386-389. 10.1038/37084.

19. Cheng, J., and Deming, T.J. (2001). Synthesis and Conformational Analysis of Optically Active Poly(β-peptides). Macromolecules *34*, 5169-5174. 10.1021/ma010386d.
20. Chen, C., Fu, H., Baumgartner, R., Song, Z., Lin, Y., and Cheng, J. (2019). Proximity-Induced Cooperative Polymerization in "Hinged" Helical Polypeptides. J. Am. Chem. Soc. *141*, 8680-8683. 10.1021/jacs.9b02298.
21. Grazon, C., Salas-Ambrosio, P., Ibarboure, E., Buol, A., Garanger, E., Grinstaff, M.W., Lecommandoux, S., and Bonduelle, C. (2020). Aqueous Ring-Opening Polymerization-Induced Self-Assembly (ROPISA) of N-Carboxyanhydrides. Angew. Chem. Int. Ed. *59*, 622-626. 10.1002/anie.201912028.
22. Rasines Mazo, A., Allison-Logan, S., Karimi, F., Chan, N.J.-A., Qiu, W., Duan, W., O'Brien-Simpson, N.M., and Qiao, G.G. (2020). Ring Opening Polymerization of α-Amino Acids: Advances in Synthesis, Architecture and Applications of Polypeptides and Their Hybrids. Chem. Soc. Rev. *49*, 4737-4834. 10.1039/C9CS00738E.
23. Thompson, M.S., Johnson, S.A., Gonsales, S.A., Brown, G.M., Kristufek, S.L., and Byers, J.A. (2023). Adding Polypeptides to the Toolbox for Redox-Switchable Polymerization and Copolymerization Catalysis. Macromolecules *56*, 3024-3035. 10.1021/acs.macromol.2c02381.
24. Quan, S.M., and Diaconescu, P.L. (2015). High Activity of an Indium Alkoxide Complex Toward Ring Opening Polymerization of Cyclic Esters. Chem. Commun. *51*, 9643 - 9646. 10.1039/C5CC01312G.
25. Wang, X., Brosmer, J.L., Thevenon, A., and Diaconescu, P.L. (2015). Highly Active Yttrium Catalysts for the Ring-Opening Polymerization of ε-Caprolactone and δ-Valerolactone. Organometallics *34*, 4700–4706. 10.1021/acs.organomet.5b00442.
26. Quan, S.M., Wang, X., Zhang, R., and Diaconescu, P.L. (2016). Redox Switchable Copolymerization of Cyclic Esters and Epoxides by a Zirconium Complex. Macromolecules *49*, 6768-6778. 10.1021/acs.macromol.6b00997.
27. Delle Chiaie, K.R., Biernesser, A.B., Ortuño, M.A., Dereli, B., Iovan, D.A., Wilding, M.J.T., Li, B., Cramer, C.J., and Byers, J.A. (2017). The Role of Ligand Redox Non-innocence in Ring-opening Polymerization Reactions Catalysed by Bis(imino)pyridine Iron Alkoxide Complexes. Dalton Trans. *46*, 12971-12980. 10.1039/C7DT03067C.
28. Lowe, M.Y., Shu, S., Quan, S.M., and Diaconescu, P.L. (2017). Investigation of Redox Switchable Titanium and Zirconium Catalysts for the Ring Opening Polymerization of Cyclic Esters and Epoxides. Inorg. Chem. Front. *4*, 1798-1805. 10.1039/C7QI00227K.
29. Quan, S.M., Wei, J., and Diaconescu, P.L. (2017). Mechanistic Studies of Redox-Switchable Copolymerization of Lactide and Cyclohexene Oxide by a Zirconium Complex. Organometallics *36*, 4451-4457. 10.1021/acs.organomet.7b00672.
30. Wei, J., Riffel, M.N., and Diaconescu, P.L. (2017). Redox Control of Aluminum Ring-Opening Polymerization: A Combined Experimental and DFT Investigation. Macromolecules *50*, 1847-1861. 10.1021/acs.macromol.6b02402.
31. Abubekerov, M., Vlček, V., Wei, J., Miehlich, M.E., Quan, S.M., Meyer, K., Neuhauser, D., and Diaconescu, P.L. (2018). Exploring Oxidation State-Dependent Selectivity in Polymerization of Cyclic Esters and Carbonates with Zinc(II) Complexes. iScience *7*, 120-131. 10.1016/j.isci.2018.08.020.
32. Abubekerov, M., Wei, J., Swartz, K.R., Xie, Z., Pei, Q., and Diaconescu, P.L. (2018). Preparation of Multiblock Copolymers via Step-wise Addition of L-lactide and Trimethylene Carbonate. Chem. Sci. *9*, 2168-2178. 10.1039/C7SC04507G.
33. Dai, R., Lai, A., Alexandrova, A.N., and Diaconescu, P.L. (2018). Geometry Change in a Series of Zirconium Compounds during Lactide Ring-Opening Polymerization. Organometallics *37*, 4040-4047. 10.1021/acs.organomet.8b00620.
34. Ortuño, M.A., Dereli, B., Chiaie, K.R.D., Biernesser, A.B., Qi, M., Byers, J.A., and Cramer, C.J. (2018). The Role of Alkoxide Initiator, Spin State, and Oxidation State in Ring-Opening Polymerization of ε-Caprolactone Catalyzed by Iron Bis(imino)pyridine Complexes. Inorg. Chem. *57*, 2064-2071. 10.1021/acs.inorgchem.7b02964.
35. Dai, R., and Diaconescu, P.L. (2019). Investigation of a Zirconium Compound for Redox Switchable Ring Opening Polymerization. Dalton Trans. *48*, 2996-3002. 10.1039/C9DT00212J.
36. Lai, A., Hern, Z.C., and Diaconescu, P.L. (2019). Switchable Ring-opening Polymerization by a Ferrocene Supported Aluminum Complex. ChemCatChem *11*, 4210-4218. 10.1002/cctc.201900747.
37. Wei, J., and Diaconescu, P.L. (2019). Redox-switchable Ring-opening Polymerization with Ferrocene Derivatives. Acc. Chem. Res. *52*, 415-424. 10.1021/acs.accounts.8b00523.
38. Deng, S., and Diaconescu, P.L. (2021). A Switchable Dimeric Yttrium Complex and Its Three Catalytic States in Ring Opening Polymerization. Inorg. Chem. Front. *8*, 2088-2096. 10.1039/D0QI01479F.
39. Qi, M., Zhang, H., Dong, Q., Li, J., Musgrave, R.A., Zhao, Y., Dulock, N., Wang, D., and Byers, J.A. (2021). Electrochemically Switchable Polymerization from Surface-anchored Molecular Catalysts. Chem. Sci. *12*, 9042-9052. 10.1039/D1SC02163J.
40. Longo, J.M., Sanford, M.J., and Coates, G.W. (2016). Ring-Opening Copolymerization of Epoxides and Cyclic Anhydrides with Discrete Metal Complexes: Structure–Property Relationships. Chem. Rev. *116*, 15167-15197. 10.1021/acs.chemrev.6b00553.
41. Fieser, M.E., Sanford, M.J., Mitchell, L.A., Dunbar, C.R., Mandal, M., Van Zee, N.J., Urness, D.M., Cramer, C.J., Coates, G.W., and Tolman, W.B. (2017).

Mechanistic Insights into the Alternating Copolymerization of Epoxides and Cyclic Anhydrides Using a (Salph)AlCl and Iminium Salt Catalytic System. J. Am. Chem. Soc. *139*, 15222-15231. 10.1021/jacs.7b09079.

42. Van Zee, N.J., and Coates, G.W. (2014). Alternating Copolymerization of Dihydrocoumarin and Epoxides Catalyzed by Chromium Salen Complexes: A New Route to Functional Polyesters. Chem. Commun. *50*, 6322-6325. 10.1039/C4CC01566E.
43. Darensbourg, D.J., Mackiewicz, R.M., Phelps, A.L., and Billodeaux, D.R. (2004). Copolymerization of CO2 and Epoxides Catalyzed by Metal Salen Complexes. Acc. Chem. Res. *37*, 836-844. 10.1021/ar030240u.
44. Lu, X.-B., Shi, L., Wang, Y.-M., Zhang, R., Zhang, Y.-J., Peng, X.-J., Zhang, Z.-C., and Li, B. (2006). Design of Highly Active Binary Catalyst Systems for CO2/Epoxide Copolymerization: Polymer Selectivity, Enantioselectivity, and Stereochemistry Control. J. Am. Chem. Soc. *128*, 1664-1674. 10.1021/ja0563830.
45. Zhu, Y., and Tao, Y. (2024). Stereoselective Ring-opening Polymerization of S-Carboxyanhydrides Using Salen Aluminum Catalysts: A Route to High-Isotactic Functionalized Polythioesters. Angew. Chem. Int. Ed. *63*, e202317305. 10.1002/anie.202317305.
46. Raman, S.K., Brulé, E., Tschan, M.J.L., and Thomas, C.M. (2014). Tandem Catalysis: A New Approach to Polypeptides and Cyclic Carbonates. Chem. Commun. *50*, 13773-13776. 10.1039/C4CC05730A.
47. Maiatska, O., Omeis, J., and Ritter, H. (2016). One-Step Approach to Amino-Functionalized Semiaromatic Polyamides: Modification and Cross-Linking. Macromolecules *49*, 737-741. 10.1021/acs.macromol.5b02368.
48. Mazo, A.R., Allison-Logan, S., Karimi, F., Chan, N.J.A., Qiu, W.L., Duan, W., O'Brien-Simpson, N.M., and Qiao, G.G. (2020). Ring Opening Polymerization of α-Amino Acids: Advances in Synthesis, Architecture and Applications of Polypeptides and Their Hybrids. Chem. Soc. Rev. *49*, 4737-4834. 10.1039/c9cs00738e.
49. Sui, Q., Borchardt, D., and Rabenstein, D.L. (2007). Kinetics and Equilibria of Cis/Trans Isomerization of Backbone Amide Bonds in Peptoids. J. Am. Chem. Soc. *129*, 12042-12048. 10.1021/ja0740925.
50. Tojo, Y., Urushibara, K., Yamamoto, S., Mori, H., Masu, H., Kudo, M., Hirano, T., Azumaya, I., Kagechika, H., and Tanatani, A. (2018). Conformational Properties of Aromatic Oligoamides Bearing Pyrrole Rings. J. Org. Chem. *83*, 4606-4617. 10.1021/acs.joc.8b00349.
51. Shepard, S.M., and Diaconescu, P.L. (2016). Redox-Switchable Hydroelementation of a Cobalt Complex Supported by a Ferrocene-Based Ligand. Organometallics *35*, 2446–2453. 10.1021/acs.organomet.6b00317.
52. Stößer, T., and Williams, C.K. (2018). Selective Polymerization Catalysis from Monomer Mixtures: Using a Commercial Cr-Salen Catalyst To Access ABA Block Polyesters. Angew. Chem. Int. Ed. *57*, 6337-6341. 10.1002/anie.201801400.
53. Van Zee, N.J., and Coates, G.W. (2015). Alternating Copolymerization of Propylene Oxide with Biorenewable Terpene-based Cyclic Anhydrides: A Sustainable Route to Aliphatic Polyesters with High Glass Transition Temperatures. Angew. Chem. Int. Ed. *127*, 2703-2706. 10.1002/anie.201410641.
54. Liu, Y., Guo, J.-Z., Lu, H.-W., Wang, H.-B., and Lu, X.-B. (2018). Making Various Degradable Polymers from Epoxides Using a Versatile Dinuclear Chromium Catalyst. Macromolecules *51*, 771-778. 10.1021/acs.macromol.7b02042.
55. Lu, X.-B., and Darensbourg, D.J. (2012). Cobalt Catalysts for the Coupling of CO2 and Epoxides to Provide Polycarbonates and Cyclic Carbonates. Chem. Soc. Rev. *41*, 1462-1484. 10.1039/C1CS15142H.
56. Liu, Y., Zhou, H., Guo, J.Z., Ren, W.M., and Lu, X.B. (2017). Completely Recyclable Monomers and Polycarbonate: Approach to Sustainable Polymers. Angew. Chem. Int. Ed. *56*, 4862-4866. 10.1002/anie.201701438.
57. Luinstra, G.A., Haas, G.R., Molnar, F., Bernhart, V., Eberhardt, R., and Rieger, B. (2005). On the Formation of Aliphatic Polycarbonates from Epoxides with Chromium(III) and Aluminum(III) Metal–Salen Complexes. Chem. Eur. J. *11*, 6298-6314. 10.1002/chem.200500356.
58. Cuartero, M., Acres, R.G., Bradley, J., Jarolimova, Z., Wang, L., Bakker, E., Crespo, G.A., and De Marco, R. (2017). Electrochemical Mechanism of Ferrocene-based Redox Molecules in Thin Film Membrane Electrodes. Electrochim. Acta *238*, 357-367. 10.1016/j.electacta.2017.04.047.
59. Darensbourg, D.J., Mackiewicz, R.M., Rodgers, J.L., Fang, C.C., Billodeaux, D.R., and Reibenspies, J.H. (2004). Cyclohexene Oxide/CO2 Copolymerization Catalyzed by Chromium(III) Salen Complexes and N-Methylimidazole: Effects of Varying Salen Ligand Substituents and Relative Cocatalyst Loading. Inorg. Chem. *43*, 6024-6034. 10.1021/ic049182e.
60. Doistau, B., Benda, L., Cantin, J.-L., Cador, O., Pointillart, F., Wernsdorfer, W., Chamoreau, L.-M., Marvaud, V., Hasenknopf, B., and Vives, G. (2020). Dual Switchable Molecular Tweezers Incorporating Anisotropic MnIII–Salphen Complexes. Dalton Trans. *49*, 8872-8882. 10.1039/D0DT01465F.
61. Veronese, L., Brivio, M., Biagini, P., Po, R., Tritto, I., Losio, S., Boggioni, L. (2020). Effect of Quaternary Phosphonium Salts as Cocatalysts on Epoxide/CO2 Copolymerization Catalyzed by salen-Type Cr(III) Complexes. Organometallics *39*, 2653-2664. 10.1021/acs.organomet.0c00269.
62. Wu, X.M., Yan, G.J., Ding, H.N., Wen, Y.Q., Guo, K.N., Zhang, X.J., Liu, B.Y. (2023). Stereoselective Copolymerization of Ring-Strained Pentacyclic Anhydride with

Cyclohexene Oxide: Cocatalyst-to-Catalyst Ratio Dependence of Polymerization Mechanism. Macromolecules *56*, 7771-7781. 10.1021/acs.macromol.3c01597.

63. Allen, S.D., Moore, D.R., Lobkovsky, E.B., Coates, G.W. (2002). High-Activity, Single-Site Catalysts for the Alternating Copolymerization of CO_2 and Propylene Oxide. J. Am. Chem. Soc. *124*, 14284-14285. 10.1021/ja028071g.
64. Lu, X.B., Liang, B., Zhang, Y.J., Tian, Y.Z., Wang, Y.M., Bai, C.X., Wang, H, Zhang, R. (2004). Asymmetric Catalysis with CO_2: Direct Synthesis of Optically Active Propylene Carbonate from Racemic Epoxides. J. Am. Chem. Soc. *126*, 3732-3733. 10.1021/ja0497345.
65. Qin, Z.Q., Thomas, C.M., Lee, S., Coates, G.W. (2003). Cobalt-Based Complexes for the Copolymerization of Propylene Oxide and CO_2: Active and Selective Catalysts for Polycarbonate Synthesis. Angew. Chem. Int. Ed. *42*, 5484-5487. 10.1002/anie.200352605.
66. Baalbaki, H.A., Roshandel, H., Hein, J.E., Mehrkhodavandi, P. (2021). Conversion of dilute CO_2 to cyclic carbonates at sub-atmospheric pressures by a simple indium catalyst. Catal. Sci. Technol. *11*, 2119-2129. 10.1039/D0CY02028A.
67. Stößer, T., Mulryan, D., and Williams, C.K. (2018). Switch Catalysis To Deliver Multi-Block Polyesters from Mixtures of Propene Oxide, Lactide, and Phthalic Anhydride. Angew. Chem. Int. Ed. *57*, 16893-16897. 10.1002/anie.201810245.
68. Van Zee, N.J., Sanford, M.J., and Coates, G.W. (2016). Electronic Effects of Aluminum Complexes in the Copolymerization of Propylene Oxide with Tricyclic Anhydrides: Access to Well-Defined, Functionalizable Aliphatic Polyesters. J. Am. Chem. Soc. *138*, 2755-2761. 10.1021/jacs.5b12888.
69. Schmid, T.E., Robert, C., Richard, V., Raman, S.K., Guérineau, V., and Thomas, C.M. (2019). Aluminum-Catalyzed One-Pot Synthesis of Polyester-b-Polypeptide Block Copolymers by Ring-Opening Polymerization. Macromol. Chem. Phys. *220*, 1900040. 10.1002/macp.201900040.
70. Robert, C., Schmid, T.E., Richard, V., Haquette, P., Raman, S.K., Rager, M.N., Gauvin, R.M., Morin, Y., Trivelli, X., Guérineau, V., et al. (2017). Mechanistic Aspects of the Polymerization of Lactide Using a Highly Efficient Aluminum(III) Catalytic System. J. Am. Chem. Soc. *139*, 6217-6225. 10.1021/jacs.7b01749.
71. Chatterjee, C., and Chisholm, M.H. (2012). Influence of the Metal (Al, Cr, and Co) and the Substituents of the Porphyrin in Controlling the Reactions Involved in the Copolymerization of Propylene Oxide and Carbon Dioxide by Porphyrin Metal(III) Complexes. 2. Chromium Chemistry. Inorg. Chem. *51*, 12041-12052. 10.1021/ic302137w.
72. Chen, X.-L., Wang, B., Song, D.-P., Pan, L., and Li, Y.-S. (2022). One-Step Synthesis of Sequence-Controlled Polyester-block-Poly(ester-alt-thioester) by Chemoselective Multicomponent Polymerization. Macromolecules *55*, 1153-1164. 10.1021/acs.macromol.1c02303.
73. Shibasaki, Y., Abe, Y., Sato, N., Fujimori, A., and Oishi, Y. (2010). Direct Condensation Polymerization of N-alkylated p-Aminobenzoic Acid and Packing of Rigid-rod Main Chains with Flexible Side Chains. Polym. J. *42*, 72-80. 10.1038/pj.2009.306.
74. Ohishi, T., Sugi, R., Yokoyama, A., and Yokozawa, T. (2006). A Variety of Poly(m-benzamide)s with Low Polydispersities from Inductive Effect-assisted Chain-growth Polycondensation. J. Polym. Sci., Part A: Polym. Chem. *44*, 4990-5003. 10.1002/pola.21616.